



Ion-beam Imaging

Proton CT

Albert Hirtl

Atominstitut, Technische Universität Wien

Advanced School on Medical Accelerators and Particle Therapy, 2 April 2019

Outline

- 1 Motivation – Why ion-beam imaging?
- 2 Introduction to imaging with ions
- 3 Summary
- 4 References

Recommended reviews on the topic:

- Robert P. Johnson (Jan. 2018). "Review of medical radiography and tomography with proton beams". In: REPORTS ON PROGRESS IN PHYSICS 81.1, p. 016701. ISSN: 0034-4885. DOI: [10.1088/1361-6633/aa8b1d](https://doi.org/10.1088/1361-6633/aa8b1d)
- G. Poludniowski, N. M. Allinson, and P. M. Evans (2015). "Proton radiography and tomography with application to proton therapy". In: BRITISH JOURNAL OF RADIOLOGY 88.1053. DOI: [10.1259/bjr.20150134](https://doi.org/10.1259/bjr.20150134)

Outline

- 1 Motivation – Why ion-beam imaging?
- 2 Introduction to imaging with ions
- 3 Summary
- 4 References

What is currently the main motivation for proton imaging?

Application in ion-beam therapy planning

Treatment plan prior to treatment

- treatment plan currently **based on computed tomography (CT)**
- basic interactions of **X-rays fundamentally different** in comparison to ions
- CT provides Hounsfield units (HUs) \Leftarrow linear attenuation coefficient
- translation of HUs to **electron densities** \Leftarrow conventional therapy
- translation of HUs to **stopping power ratio (SPR)** \Leftarrow ion-beam therapy

photon therapy

$$HU = 1000 \times \frac{\mu - \mu_{\text{water}}}{\mu_{\text{water}}}$$

$$I = I_0 e^{-\mu x}$$

ion-beam therapy

$$\bar{R}(E_0) = \int_{E_0}^0 \frac{1}{S(E)} dE \quad \text{with} \quad S(E) = -\frac{dE}{dx}$$

Treatment plan prior to treatment

- treatment plan currently **based on CT**
- basic interactions of **X-rays fundamentally different** in comparison to ions
- CT provides HUs \Leftarrow **linear attenuation coefficient**
- translation of HUs to **electron densities** \Leftarrow **conventional therapy**
- translation of HUs to **SPR** \Leftarrow **ion-beam therapy**

HU to SPR calibration curve is required:

- **calibration curve required for each CT scanner used for treatment planning**
- accuracy of curve important for accuracy of dose calculation
- **simplest calibration curve** obtained by **measurements of HUs and SPR of known tissue substitutes**
 - ▶ is sensitive to the used tissue substitute
- less sensitive method required \Rightarrow **stoichiometric calibration**

Treatment plan prior to treatment

- treatment plan currently **based on CT**
- basic interactions of **X-rays fundamentally different** in comparison to ions
- CT provides HUs \Leftarrow **linear attenuation coefficient**
- translation of HUs to **electron densities** \Leftarrow **conventional therapy**
- translation of HUs to **SPR** \Leftarrow **ion-beam therapy**

Stoichiometric calibration:

- introduced by Schneider, Pedroni, and Lomax (1996)
- based on **theoretical HUs and SPRs** of human body tissue
 - ▶ calculated according to known **elemental composition of human tissue**
 - ▶ and **CT-specific parameters** determined in **measurements of tissue substitutes**
- method less sensitive to the used tissue substitutes

HUs to stopping power ratio calibration curve

Coarse recipe for stoichiometric calibration:

- 1 scan tissue substitutes of known chemical composition with CT used for treatment planning \Rightarrow HUs
- 2 determine scanner-specific parameters based on HUs measurement \Rightarrow *E*-dependence of attenuation
 - ▶ total attenuation coefficient of mixtures can be written with energy dependent coefficients K (i. e. cross sections)

$$\mu = \rho N_g(Z, A) \left[K^{\text{ph}} \tilde{Z}^{3.62} + K^{\text{coh}} \hat{Z}^{1.86} + K^{\text{NN}} \right]$$

ρN_g ... electron density, K^{NN} ... Klein-Nishina cross section, \tilde{Z}, \hat{Z} ... for mixtures

- 3 calculate HU for human tissue (ICRP) using the previous CT calibration \Rightarrow $\text{HU} \propto \mu$
- 4 calculate SPR for human tissue ($\propto \rho N_g$)
- 5 plot HU versus SPR
- 6 determine calibration curve by fitting through the data points

\Rightarrow there can be ambiguities!

\Rightarrow all details in Schneider, Pedroni, and Lomax (1996)

Conversion errors

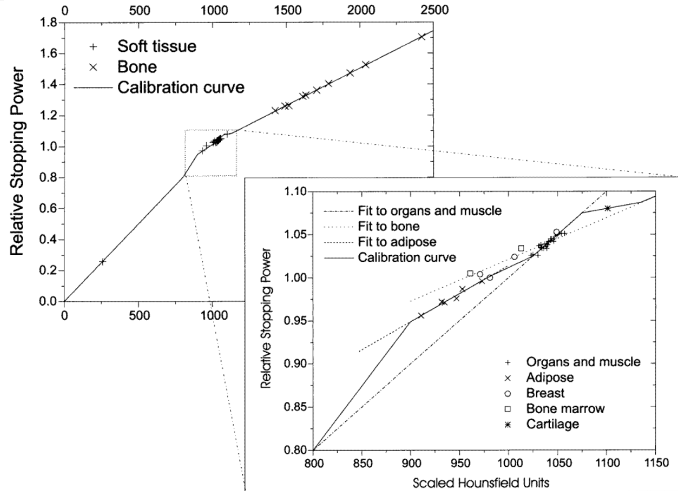


Image: Schaffner and Pedroni (1998)

Errors & ambiguities:

- Conversion HU → stopping power
 - ▶ Introduces conversion errors
 - ▶ Material-dependent ambiguities
 - ▶ points for bone on straight line
 - ▶ no unique calibration for soft tissue

Range errors are an issue:

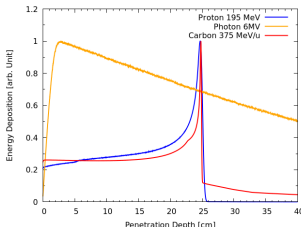


Image: Courtesy of H. Fuchs

Conversion errors

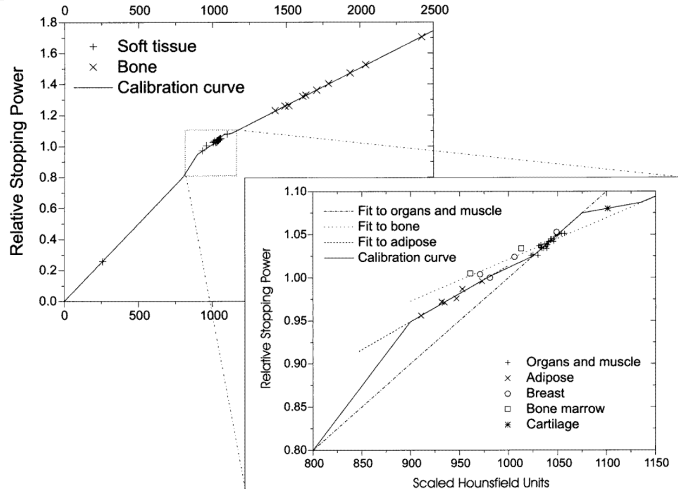


Image: Schaffner and Pedroni (1998)

Errors & ambiguities:

- Conversion HU → stopping power
 - ▶ Introduces conversion errors
 - ▶ Material-dependent ambiguities
 - ▶ points for bone on straight line
 - ▶ no unique calibration for soft tissue

Range errors are an issue:

- ≈ 1.8% for bone
 - ≈ 1.1% for soft tissue
 - can be substantially larger in the presence of high Z materials!

⇒ see Poludniowski, Allinson, and Evans (2015) or Robert P. Johnson (2018)

Known facts

- energy deposition (\approx dose) in ion-beam therapy **strongly localised**

Known facts

- energy deposition (\approx dose) in ion-beam therapy **strongly localised**
- wrong determination of SPR might lead to **deposition** of maximum dose **outside of target** region

Known facts

- energy deposition (\approx dose) in ion-beam therapy **strongly localised**
- **wrong determination of SPR** might lead to **deposition** of maximum dose **outside of target** region

Accurate determination of SPR very important!

Outline

1 Motivation – Why ion-beam imaging?

2 Introduction to imaging with ions

3 Summary

4 References

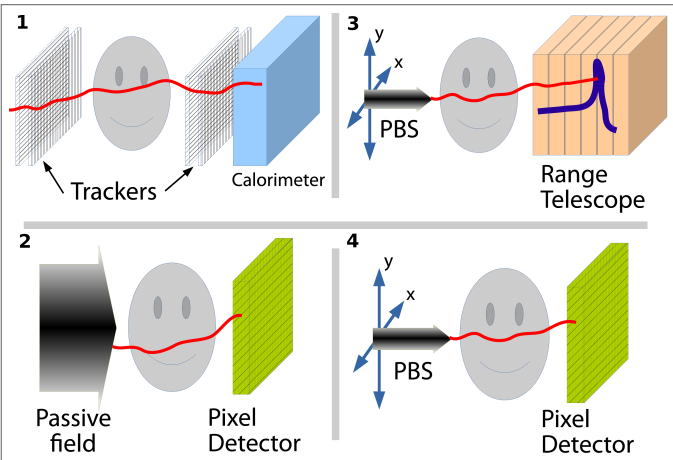
Basic considerations in tomographic imaging:

- projections need to be acquired, either by
 - 1 rotation of patient around its vertical axis ⇒ positioning?
 - 2 rotation of nozzle with imaging system around patient ⇒ gantry?
- projections used as input in a tomographic reconstruction algorithm
- ions need to pass through the imaged object ⇒ higher energies than for therapy
- energy loss of transmitted protons in object ⇒ image contrast

Information required for SPR reconstruction:

- path of ions traversing object ⇒ can only be estimated
 - ▶ achieved by particle tracking
 - energy loss of ions in object ⇒ measurement of residual energy
 - ▶ achieved by using a calorimeter
- ⇒ different ways to achieve fully or partially

Types of set-ups



Four types:

- 1** single particle tracking
 - ▶ tomography
 - ▶ tracking challenging \Rightarrow fluence!
- 2** passive field + pixel detector
 - ▶ energy variation \Rightarrow radiography
- 3** scanning + range telescope
 - ▶ energy variation \Rightarrow radiography
- 4** scanning + pixel detector
 - ▶ radiography & tomography
 - ▶ ion entry position roughly known

Image: Krah et al. (2018)

The physics principle in ion-beam therapy summarised

- continuous **energy loss (ΔE)** of a particle traversing matter

The physics principle in ion-beam therapy summarised

- continuous **energy loss (ΔE)** of a particle traversing matter
- energy loss given by the **mass stopping power $S \Rightarrow$ Bethe-Bloch**

$$\frac{S}{\rho} = -\frac{1}{\rho} \frac{dE}{dx}$$

The physics principle in ion-beam therapy summarised

- continuous **energy loss (ΔE)** of a particle traversing matter
- energy loss given by the **mass stopping power S** ⇒ Bethe-Bloch

$$\frac{S}{\rho} = -\frac{1}{\rho} \frac{dE}{dx}$$

- **maximum deposition** of energy at the end of the particle's path ⇒ Bragg peak

The physics principle in ion-beam therapy summarised

- continuous **energy loss** (ΔE) of a particle traversing matter
- energy loss given by the **mass stopping power** $S \Rightarrow$ Bethe-Bloch

$$\frac{S}{\rho} = -\frac{1}{\rho} \frac{dE}{dx}$$

- **maximum deposition** of energy at the end of the particle's path \Rightarrow Bragg peak
- given by **mean range**, R , of a particle with given energy E_0

$$R(E_0) = \int_{E_0}^0 \frac{1}{S(E)} dE = \int_{E_0}^0 \left(-\frac{dE}{dx} \right)^{-1} dE$$

The physics principle in ion-beam therapy summarised

- continuous **energy loss (ΔE)** of a particle traversing matter
- energy loss given by the **mass stopping power S** ⇒ Bethe-Bloch

$$\frac{S}{\rho} = -\frac{1}{\rho} \frac{dE}{dx}$$

- **maximum deposition** of energy at the end of the particle's path ⇒ Bragg peak
- given by **mean range, R** , of a particle with given energy E_0

$$R(E_0) = \int_{E_0}^0 \frac{1}{S(E)} dE = \int_{E_0}^0 \left(-\frac{dE}{dx} \right)^{-1} dE$$

⇒ if $\frac{dE}{dx}$ wrong ⇒ $R(E)$ wrong ⇒ wrong dose deposition

Energy loss in object

- integral over specific energy loss $\frac{dE}{ds}$ along track length s

$$\Delta E = \int \frac{dE}{ds} ds = \int \frac{dE}{dx} dx \approx \sum \rho(s) \frac{dE}{dx} \Delta s$$

$\frac{dE}{dx}$ is the energy loss per unit density-weighted track length $x = \rho \cdot s$

- $\frac{dE}{dx}$ only weak dependence on traversed material: $\frac{dE}{dx} \sim \frac{Z}{A}$

Energy loss in object

- integral over specific energy loss $\frac{dE}{ds}$ along track length s

$$\Delta E = \int \frac{dE}{ds} ds = \int \frac{dE}{dx} dx \approx \sum \rho(s) \frac{dE}{dx} \Delta s$$

$\frac{dE}{dx}$ is the energy loss per unit density-weighted track length $x = \rho \cdot s$

- $\frac{dE}{dx}$ only weak dependence on traversed material: $\frac{dE}{dx} \sim \frac{Z}{A}$

⇒ measurement of ΔE gives $\rho(s)$ in traversed object ⇐

What about the ion path inside the object?

Ions undergo multiple Coulomb scattering (MCS)

- the scattering angle Θ_{MCS} is energy and material dependent

$$\Theta_{\text{MCS}} \approx \frac{13.6 \text{ MeV}}{\beta p} z \sqrt{I/X_0}$$

with the radiation length (material constant) X_0 , and $z = 1$ for protons

- for 250MeV protons traversing 20cm of water $\Theta_{\text{MCS}} \approx 1^\circ$
- **displacement** of protons due to MCS

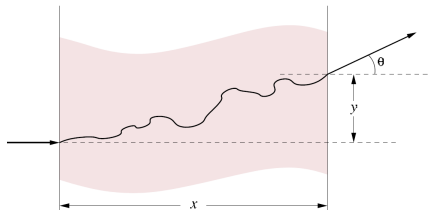


Image: Williams (2004)

⇒ measurement / determination / calculation of

- energy loss of ions in object
- most likely path of protons in object

⇒ measurement / determination / calculation of

- energy loss of ions in object
- most likely path of protons in object

Energy loss ΔE :

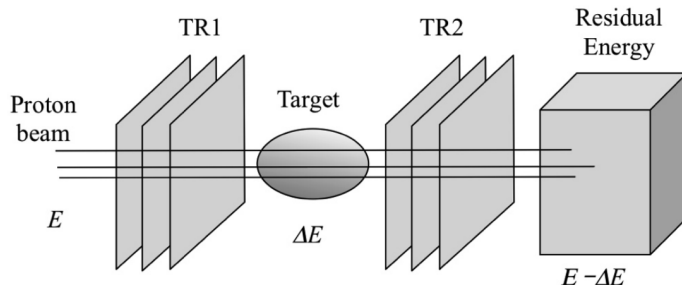


Image: Bucciantonio (2015)

⇒ measurement / determination / calculation of

- energy loss of ions in object
- most likely path of protons in object

ΔE and MCS:

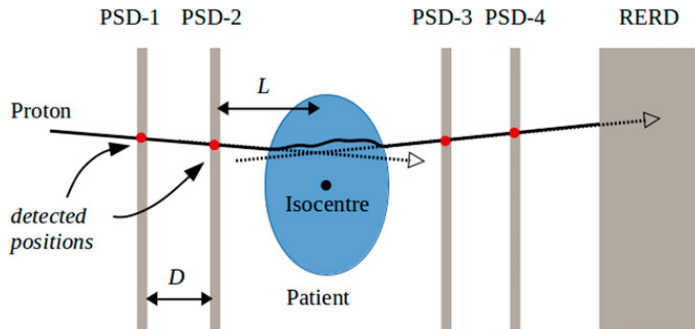


Image: Poludniowski, Allinson, and Evans (2015)

Reconstructing the SP-“image” – Algebraic reconstruction technique (ART)

→ **start** from linear stopping power $S(x, y, E)$

$$- dE = S(x, y, E) dl \quad (1)$$

dE ... differential energy loss of particle with E in a point (x, y) in a slice along a path dl

Reconstructing the SP-“image” – Algebraic reconstruction technique (ART)

- start from linear stopping power $S(x, y, E)$

$$- dE = S(x, y, E) dl \quad (1)$$

dE ... differential energy loss of particle with E in a point (x, y) in a slice along a path dl

- separate energy and material factors from SP

$$\text{linear SP} = \text{mass SP} \times \text{physical density}$$

Reconstructing the SP-“image” – Algebraic reconstruction technique (ART)

- start from linear stopping power $S(x, y, E)$

$$- dE = S(x, y, E) dl \quad (1)$$

dE ... differential energy loss of particle with E in a point (x, y) in a slice along a path dl

- separate energy and material factors from SP

$$\text{linear SP} = \text{mass SP} \times \text{physical density}$$

- rewriting with mass SP ($\frac{S}{\rho}(x, y, E) = S(x, y, E)/\rho(x, y)$) and multiplying both sides of eq. (1) with mass SP at some reference energy E_0

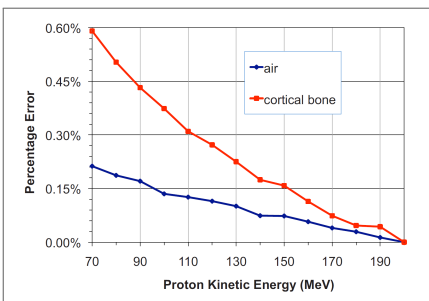
$$- \frac{S}{\rho}(x, y, E_0) dE = \frac{S}{\rho}(x, y, E_0) \cdot \frac{S}{\rho}(x, y, E) \cdot \rho(x, y) dl \quad (2)$$

E_0 ... reference energy (arbitrary, e. g. energy of protons from accelerator)

Reconstructing the “image” ctd.

→ divide by mass SP at E ⇒ SPR

$$\frac{\frac{S}{\rho}(x, y, E_0)}{\frac{S}{\rho}(x, y, E)} dE = S(x, y, E_0) dI \quad (3)$$



- ▶ mass SPR of materials in figure left compared to mass SPR of water with $E_0 = 200\text{MeV}$ (from NIST)
 - ▶ mass SPR error at E_0 to E in eq. (3) over a wide energy range is $< 6 \cdot 10^{-3}$
 - ▶ \Rightarrow small dependence on material
 - ▶ \Rightarrow approximated with measured SPR for liquid water

Reconstructing the “image” ctd.

→ with the SPR of water

$$-\left[\frac{S}{\rho}(\text{H}_2\text{O})\right]_E^{E_0} dE = S(x, y, E_0) dl \quad (4)$$

with the abbreviation

$$\left[\frac{S}{\rho}(\text{H}_2\text{O})\right]_E^{E_0} \cong \left[\frac{S}{\rho}(x, y)\right]_E^{E_0} = \frac{\frac{S}{\rho}(x, y, E_0)}{\frac{S}{\rho}(x, y, E)}$$

Reconstructing the “image” ctd.

- with the SPR of water

$$-\left[\frac{S}{\rho}(\text{H}_2\text{O})\right]_E^{E_0} dE = S(x, y, E_0) dl \quad (4)$$

with the abbreviation

$$\left[\frac{S}{\rho}(\text{H}_2\text{O})\right]_E^{E_0} \cong \left[\frac{S}{\rho}(x, y)\right]_E^{E_0} = \frac{\frac{S}{\rho}(x, y, E_0)}{\frac{S}{\rho}(x, y, E)}$$

- $S(x, y, E_0)$ in eq. (4): SP at reference energy E_0 in the reconstruction plane

Reconstructing the “image” ctd.

- with the SPR of water

$$-\left[\frac{S}{\rho}(\text{H}_2\text{O})\right]_E^{E_0} dE = S(x, y, E_0) dl \quad (4)$$

with the abbreviation

$$\left[\frac{S}{\rho}(\text{H}_2\text{O})\right]_E^{E_0} \cong \left[\frac{S}{\rho}(x, y)\right]_E^{E_0} = \frac{\frac{S}{\rho}(x, y, E_0)}{\frac{S}{\rho}(x, y, E)}$$

- $S(x, y, E_0)$ in eq. (4): SP at reference energy E_0 in the reconstruction plane
- integrating both sides in eq. (4) along proton path yields

$$-\int_{E_{\text{in}}}^{E_{\text{out}}} \left[\frac{S}{\rho}(\text{H}_2\text{O})\right]_E^{E_0} dE = \int_L S(x, y, E_0) dl \quad (5)$$

Projection equation for SP image at E_0

$$-\int_{E_{\text{in}}}^{E_{\text{out}}} \left[\frac{S}{\rho} (\text{H}_2\text{O}) \right]_E^{E_0} dE = \int_L S(x, y, E_0) dl \quad (6)$$

the SP for $E_0 = E_{\text{in}}$ at any point in the reconstruction plane can be determined

⇒ choice of E_0 arbitrary!

⇒ L proton path in object (MLP!)

Projection equation for SP image at E_0

$$-\int_{E_{\text{in}}}^{E_{\text{out}}} \left[\frac{S}{\rho} (\text{H}_2\text{O}) \right]_E^{E_0} dE = \int_L S(x, y, E_0) dl \quad (6)$$

the SP for $E_0 = E_{\text{in}}$ at any point in the reconstruction plane can be determined

\Rightarrow choice of E_0 arbitrary!

$\Rightarrow L$ proton path in object (MLP!)

Discretisation of object (phantom) in N pixels \Rightarrow projection equation for pixel j for M protons:

$$p_i \equiv - \int_{E_{\text{in}}}^{E_{\text{out}}} \left[\frac{S}{\rho} (\text{H}_2\text{O}) \right]_E^{E_0} dE = \sum_{j=1}^N w_{ij} S_j(E_0) \quad i = 1, \dots, M \quad (7)$$

p_i is the measured energy loss (ray sum) and w_{ij} is the path length of the proton i through pixel j

Projection equation for SP image at E_0

$$-\int_{E_{\text{in}}}^{E_{\text{out}}} \left[\frac{S}{\rho} (\text{H}_2\text{O}) \right]_E^{E_0} dE = \int_L S(x, y, E_0) dl \quad (6)$$

the SP for $E_0 = E_{\text{in}}$ at any point in the reconstruction plane can be determined

\Rightarrow choice of E_0 arbitrary!

$\Rightarrow L$ proton path in object (MLP!)

Discretisation of object (phantom) in N pixels \Rightarrow projection equation for pixel j for M protons:

$$p_i \equiv - \int_{E_{\text{in}}}^{E_{\text{out}}} \left[\frac{S}{\rho} (\text{H}_2\text{O}) \right]_E^{E_0} dE = \sum_{j=1}^N w_{ij} S_j(E_0) \quad i = 1, \dots, M \quad (7)$$

p_i is the measured energy loss (ray sum) and w_{ij} is the path length of the proton i through pixel j

p_i is the energy loss (\equiv ray sum) \Rightarrow measured with the calorimeter

Projection equation for SP image at E_0

$$-\int_{E_{\text{in}}}^{E_{\text{out}}} \left[\frac{S}{\rho} (\text{H}_2\text{O}) \right]_E^{E_0} dE = \int_L S(x, y, E_0) dl \quad (6)$$

the SP for $E_0 = E_{\text{in}}$ at any point in the reconstruction plane can be determined

\Rightarrow choice of E_0 arbitrary!

$\Rightarrow L$ proton path in object (MLP!)

Discretisation of object (phantom) in N pixels \Rightarrow projection equation for pixel j for M protons:

$$p_i \equiv - \int_{E_{\text{in}}}^{E_{\text{out}}} \left[\frac{S}{\rho} (\text{H}_2\text{O}) \right]_E^{E_0} dE = \sum_{j=1}^N w_{ij} S_j(E_0) \quad i = 1, \dots, M \quad (7)$$

p_i is the measured energy loss (ray sum) and w_{ij} is the path length of the proton i through pixel j

reconstruction problem reduced to solving a linear eq. for $S_j(E_0)$

\Rightarrow details see Wang, Mackie, and Tome (2010) or Civinini et al. (2017)

Statistical variations influencing the resolution:

lateral straggling, σ_x : lateral position at given depth ← MCS

angular straggling, σ_Θ : proton direction at given depth ← MCS

energy straggling, σ_E : energy at given depth ← Bethe-Bloch

range straggling, σ_R : stopping depth for a given energy ← Bethe-Bloch

Statistical variations influencing the resolution:

lateral straggling, σ_x : lateral position at given depth ← MCS

angular straggling, σ_Θ : proton direction at given depth ← MCS

energy straggling, σ_E : energy at given depth ← Bethe-Bloch

range straggling, σ_R : stopping depth for a given energy ← Bethe-Bloch

In addition:

inelastic nuclear interactions: removal of proton

Statistical variations influencing the resolution:

lateral straggling, σ_x : lateral position at given depth ← MCS

angular straggling, σ_θ : proton direction at given depth ← MCS

energy straggling, σ_E : energy at given depth ← Bethe-Bloch

range straggling, σ_R : stopping depth for a given energy ← Bethe-Bloch

A few numbers:

Depth (cm)	200-MeV proton incident on water				
	σ_x (cm)	σ_θ (mrad)	σ_E (MeV)	E_m (MeV)	σ_R (cm)
5	0.04	15	0.8	176.6	—
10	0.11	20	1.2	150.9	—
20	0.37	41	2.2	86.3	—
At range	—	—	—		0.29

Table: Poludniowski, Allinson, and Evans (2015)

Situation can be influenced!

lateral and angular straggling

- is reduced at higher energies ⇒ degradation of image contrast
- is reduced for heavier ions (carbon, helium)

lateral and angular straggling

- is reduced at higher energies ⇒ degradation of image contrast
- is reduced for heavier ions (carbon, helium)

energy and range straggling

- is a kind of noise
- can be reduced by increasing the number of protons

lateral and angular straggling

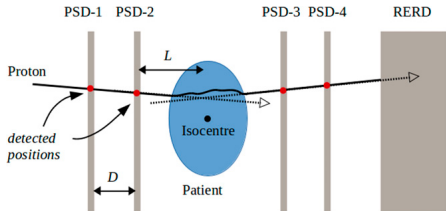
- is reduced at higher energies ⇒ degradation of image contrast
- is reduced for heavier ions (carbon, helium)

energy and range straggling

- is a kind of noise
- can be reduced by increasing the number of protons

What are the technological constraints for an appropriate application?

General tracking set-up:



PSD: position-sensitive detector
RERD: residual energy-range detector

Constraints for potential set-up:

Design feature	Constraint value	LLU/UCSC/NIU prototype system
Number of PSDs, N	$N = 4$	4
PSD pitch, P	$\frac{P}{\sqrt{12}} < 1 \text{ mm}$	0.1 mm
PSD offsets, L/D	$\frac{PL}{\sqrt{6}D} < 1 \text{ mm}$	0.5 mm
PSD thickness, T	$0.1L\sqrt{\frac{T}{X_0}} < 1 \text{ mm}$	1.4 mm
RERD discretization, Δ (range telescope)	$\frac{4}{\sqrt{12}} < 3 \text{ mm water-equivalent}$	–
RERD energy resolution, σ_E/E (calorimeter)	$< 0.6\%$ (200 MeV)	0.3% (200 MeV) ⁵⁰

Image and Table: Poludniowski, Allinson, and Evans (2015)

Requirements for an appropriate system for proton therapy

Category	Parameter	Value
Proton beam	Energy	$\geq 200 \text{ MeV}$ (head)
		$\geq 250 \text{ MeV}$ (body)
	Flux ^a	$\geq 3000 \text{ protons cm}^{-2} \text{ s}^{-2}$
Imaging dose	Maximum absorbed dose ^b	$< 20 \text{ mGy}$
Image quality	Spatial resolution, σ	$\approx 1 \text{ mm}$
	Relative stopping-power accuracy	$< 1\%$
Time	Data acquisition time	$< 10 \text{ min}$
	Reconstruction time	$< 10 \text{ min}$

Table: Poludniowski, Allinson, and Evans (2015)

⇒ proton energy beyond 250MeV would allow the imaging of extended objects!

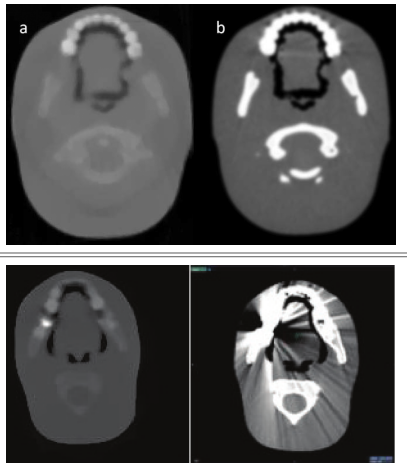
Non-exhaustive overview of active groups

Group	Year of reference	Area (cm ²)	Position-sensitive detector technology (number of units)	Residual energy-range detector technology	Proton rate (Hz)	pCT or pRG
Paul Scherrer Institute ⁴³	2005	22.0 × 3.2	x-y Sci-Fi (2)	Plastic scintillator telescope	1 M ^a	pRG
LLU/UCSC/NIU ⁶	2013	17.4 × 9.0	x-y SiSDs (4)	CsI (Tl) calorimeters	15 k ^a	pCT
LLU/UCSC/CSUSB ⁵⁵	2014	36.0 × 9.0	x-y SiSDs (4)	Plastic scintillator hybrid telescope	2 M ^a	pCT
AQUA ⁵⁹	2013	30.0 × 30.0	x-y GEMs (2)	Plastic scintillator telescope	1 M ^a	pRG
PRIMA I ⁶⁶	2014	5.1 × 5.1	x-y SiSDs (4)	YAG:Ce calorimeters	10 k ^a	pCT
PRIMA II ⁶⁶	2014	20.0 × 5.0	x-y SiSDs (4)	YAG:Ce calorimeters	1 M	pCT
INFN ⁶⁹	2014	30 × 30	x-y Sci-Fi (4)	x-y Sci-Fi	1 M	pCT
NIU/FNAL ⁷⁰	2014	24.0 × 20.0	x-y Sci-Fi (4)	Plastic scintillator telescope	2 M	pCT
Niigata University ⁷¹	2014	9.0 × 9.0	x-y SiSDs (4)	NaI(Tl) calorimeter	30 ^a	pCT
PRaVDA ⁷²	2015	9.5 × 95	x-u-v SiSDs (4)	CMOS APS telescope	1 M	pCT

Table: Poludniowski, Allinson, and Evans (2015)

Proton computed tomography (pCT) – examples

pCT vs X-ray:



pCT slices ($E_p \approx 62\text{MeV}$):

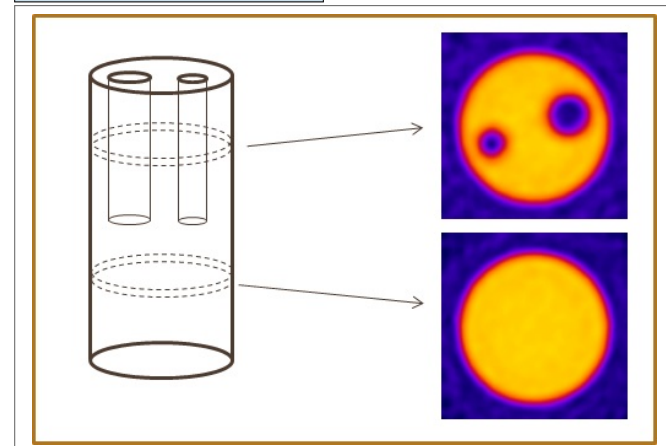
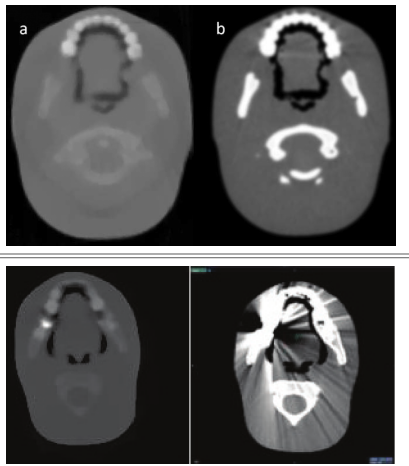


Image: Scaringella et al. 2014

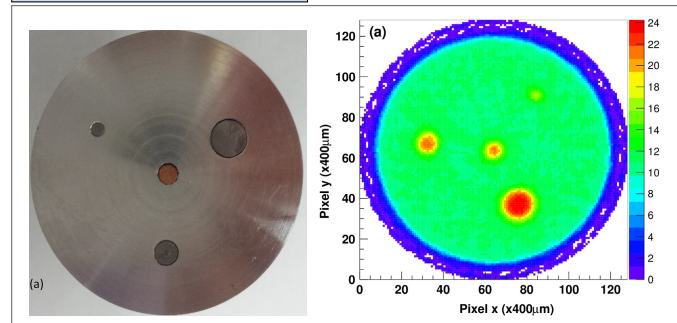
Images: R. P. Johnson et al. 2016 (top), Ordóñez et al. 2017 (bottom)

Proton computed tomography (pCT) – examples

pCT vs X-ray:



SP map ($E_p \approx 175\text{MeV}$):



Images: Bruzzi et al. 2017

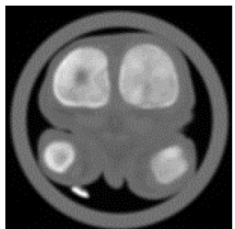
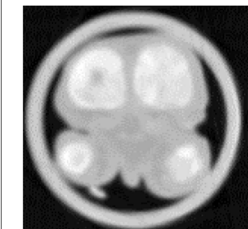
Images: R. P. Johnson et al. 2016 (top), Ordonez et al. 2017 (bottom)

Ion-beam computed tomography (iCT) – examples

Sample:



iCT vs X-ray:



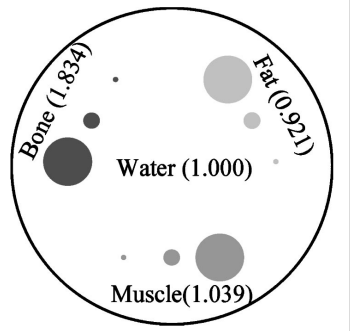
Images: Shinoda, Kanai, and Kohno 2006

- less MCS for ions like carbon
- fragments need to be considered
- helium is an interesting option

Dose considerations:

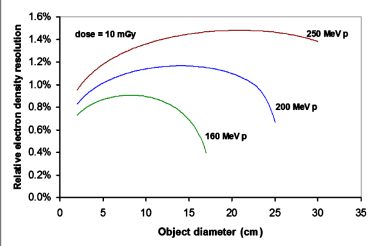
- dose deposition due to ion-beam imaging low (estimated to a few mGy for a pCT head scan)
⇒ Schulte et al. (2005)
- typical head scan of diagnostic x-ray CT up to $\approx 40\text{mGy}$

Phantom:



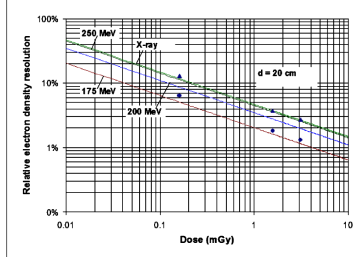
Images: Schulte et al. (2005)

Resolution vs. diameter:



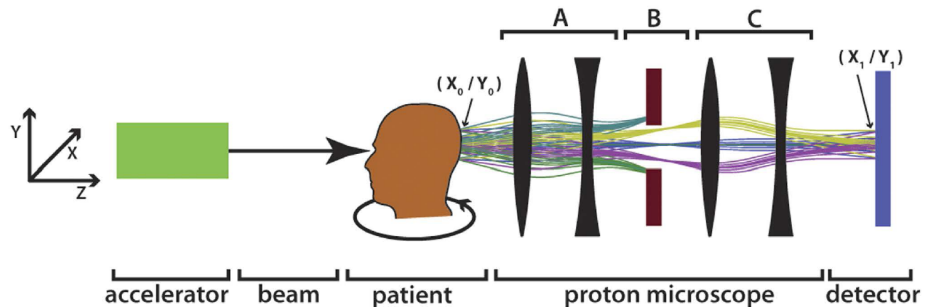
⇒ for 10mGy at the centre

Resolution vs. dose:



Other interesting imaging options with ions

PRIOR – Proton Microscope for FAIR (GeV protons)



⇒ sub-millimetre resolution

⇒ biological samples with 0.8GeV protons

Image: Prall, Durante, et al. (2016)

PRIOR – Proton Microscope for FAIR (0.8GeV protons)

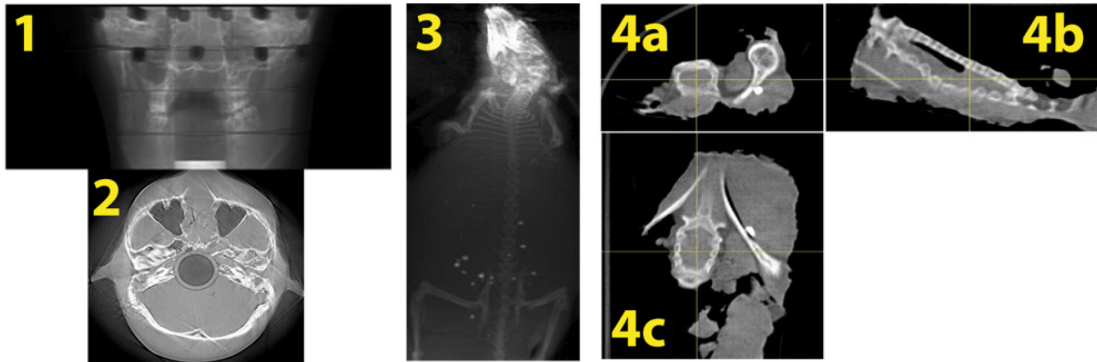
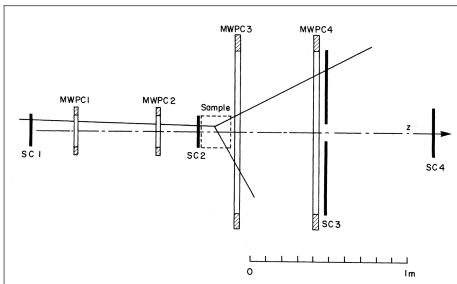
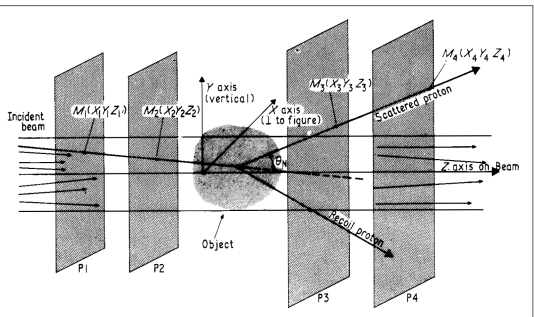


Image: Prall, Lang, et al. (2015)

The nuclear option – Nuclear scattering radiography ($\approx 1\text{GeV}$ protons)



Images: SAUDINOS et al. (1975) and CHARPAK et al. (1979)

- most protons pass object and undergo MCS (e. m.) ⇐ small angles
- some elastic (pp) and quasi-elastic (pN) scattering ⇐ large angles
- point of scattering: **intersection of incident and scattered trajectories**
- **3D reconstruction of density variations in object with one exposure!**
- is **not correlated to the number of electrons** \Rightarrow **no SP!!**

Nuclear scattering radiography of electric motor

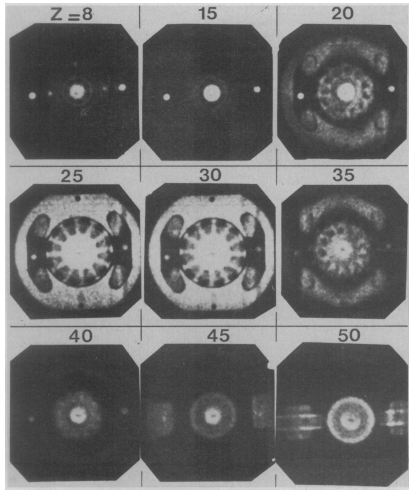


Image: DUCHAZE AUBENEIX et al. (1983)

Outline

- 1 Motivation – Why ion-beam imaging?
- 2 Introduction to imaging with ions
- 3 Summary
- 4 References

Summary

Pros

- direct measurement of SPR with iCT **⇒ no extrapolation**
- improvement in treatment planning **⇒ smaller safety margins**
- less dose to the patient than with diagnostic x-ray CT

Challenges (many!)

- clinical particle fluence **⇒ fast detectors required**
- positioning of patients **⇒ gantry?**
- MCS **⇒ higher energies?**

Thank you for your attention!

Outline

- 1 Motivation – Why ion-beam imaging?
- 2 Introduction to imaging with ions
- 3 Summary
- 4 References

References I

- Bruzzi, M. et al. (2017). "Proton computed tomography images with algebraic reconstruction". In: Nuclear Instruments and Methods in Physics Research Section A: Accelerators, Spectrometers, Detectors and Associated Equipment 845. Proceedings of the Vienna Conference on Instrumentation 2016, pp. 652–655. ISSN: 0168-9002. DOI: <https://doi.org/10.1016/j.nima.2016.05.056>. URL: <http://www.sciencedirect.com/science/article/pii/S0168900216304454>.
- Bucciantonio, Martina (2015). "Development of an advanced Proton Range Radiography system for hadrontherapy". PhD thesis. Universität Bern.
- CHARPAK, G et al. (1979). "PROGRESS IN NUCLEAR-SCATTERING RADIOGRAPHY". In: IEEE TRANSACTIONS ON NUCLEAR SCIENCE 26.1, 654–657. DOI: 10.1109/TNS.1979.4329703.
- Civinini, C. et al. (JAN 2017). "Proton Computed Tomography: iterative image reconstruction and dose evaluation". In: JOURNAL OF INSTRUMENTATION 12. 18th International Workshop on Radiation Imaging Detectors, Barcelona, SPAIN, JUL 03-07, 2016. DOI: 10.1088/1748-0221/12/01/C01034.
- DUCHAZE AUBENEIX, JC et al. (1983). "PROTON NUCLEAR-SCATTERING RADIOGRAPHY". In: IEEE TRANSACTIONS ON NUCLEAR SCIENCE 30.1, 601–604. DOI: 10.1109/TNS.1983.4332341.
- Johnson, R. P. et al. (Feb. 2016). "A Fast Experimental Scanner for Proton CT: Technical Performance and First Experience With Phantom Scans". In: IEEE Transactions on Nuclear Science 63.1, pp. 52–60. ISSN: 0018-9499. DOI: 10.1109/TNS.2015.2491918.
- Johnson, Robert P. (Jan. 2018). "Review of medical radiography and tomography with proton beams". In: REPORTS ON PROGRESS IN PHYSICS 81.1, p. 016701. ISSN: 0034-4885. DOI: 10.1088/1361-6633/aae514.

References II

- Krah, N. et al. (JUL 2018). "A comprehensive theoretical comparison of proton imaging set-ups in terms of spatial resolution". In: **PHYSICS IN MEDICINE AND BIOLOGY** 63.13. ISSN: 0031-9155. DOI: 10.1088/1361-6560/aaca1f.
- Ordonez, Caesar E. et al. (2017). "A Real-time Image Reconstruction System for Particle Treatment Planning Using Proton Computed Tomography (pCT)". In: **CONFERENCE ON THE APPLICATION OF ACCELERATORS IN RESEARCH AND INDUSTRY (CAARI 2016)**. Ed. by Parriott, C. Vol. 90. Physics Procedia. 24th International Conference on the Application of Accelerators in Research and Industry (CAARI), Fort Worth, TX, OCT 30-NOV 04, 2016. Los Alamos Natl Lab; Sandia Natl Labs; Univ N Texas, 193–199. DOI: 10.1016/j.phpro.2017.09.058.
- Poludniowski, G., N. M. Allinson, and P. M. Evans (2015). "Proton radiography and tomography with application to proton therapy". In: **BRITISH JOURNAL OF RADIOLOGY** 88.1053. DOI: 10.1259/bjr.20150134.
- Prall, M., M. Durante, et al. (JUN 10 2016). "High-energy proton imaging for biomedical applications". In: **SCIENTIFIC REPORTS** 6. ISSN: 2045-2322. DOI: 10.1038/srep27651.
- Prall, M., P. M. Lang, et al. (2015). "Towards Proton Therapy and Radiography at FAIR". In: **FAIRNESS 2014: FAIR NEXT GENERATION SCIENTISTS 2014**. Vol. 599. Journal of Physics Conference Series. 3rd Workshop on FAIRNESS - FAIR Next Generation ScientistS, Vietri sul Mare, ITALY, SEP 22-27, 2014. DOI: 10.1088/1742-6596/599/1/012041.
- SAUDINOS, J et al. (1975). "NUCLEAR SCATTERING APPLIED TO RADIOGRAPHY". In: **PHYSICS IN MEDICINE AND BIOLOGY** 20.6, 890–905. DOI: 10.1088/0031-9155/20/6/002.

References III

- Scaringella, M. et al. (DEC 2014). "A proton Computed Tomography based medical imaging system". In: JOURNAL OF INSTRUMENTATION 9. DOI: [10.1088/1748-0221/9/12/C12009](https://doi.org/10.1088/1748-0221/9/12/C12009).
- Schaffner, B and E Pedroni (1998). "The precision of proton range calculations in proton radiotherapy treatment planning: experimental verification of the relation between CT-HU and proton stopping power". In: Physics in Medicine & Biology 43.6, p. 1579. DOI: [10.1088/0031-9155/43/6/016](https://doi.org/10.1088/0031-9155/43/6/016).
- Schneider, U, E Pedroni, and A Lomax (JAN 1996). "The calibration of CT Hounsfield units for radiotherapy treatment planning". In: PHYSICS IN MEDICINE AND BIOLOGY 41.1, 111–124. DOI: [10.1088/0031-9155/41/1/009](https://doi.org/10.1088/0031-9155/41/1/009).
- Schulte, Reinhard W. et al. (2005). "Density resolution of proton computed tomography". In: Medical Physics 32.4, pp. 1035–1046. DOI: [10.1118/1.1884906](https://doi.org/10.1118/1.1884906). eprint:
<https://aapm.onlinelibrary.wiley.com/doi/pdf/10.1118/1.1884906>. URL:
<https://aapm.onlinelibrary.wiley.com/doi/abs/10.1118/1.1884906>.
- Shinoda, Hiroshi, Tatsuaki Kanai, and Toshiyuki Kohno (2006). "Application of heavy-ion CT". In: Physics in Medicine & Biology 51.16, p. 4073. URL: <http://stacks.iop.org/0031-9155/51/i=16/a=013>.
- Wang, Dongxu, T. Rockwell Mackie, and Wolfgang A. Tome (AUG 2010). "On the use of a proton path probability map for proton computed tomography reconstruction". In: MEDICAL PHYSICS 37.8, 4138–4145. DOI: [10.1118/1.3453767](https://doi.org/10.1118/1.3453767).
- Williams, DC (JUL 7 2004). "The most likely path of an energetic charged particle through a uniform medium". In: PHYSICS IN MEDICINE AND BIOLOGY 49.13, 2899–2911. DOI: [10.1088/0031-9155/49/13/010](https://doi.org/10.1088/0031-9155/49/13/010).